

**Evidence for a narrow  $D_{03}$  state in  $K^- p \rightarrow \eta\Lambda$  near threshold**Bo-Chao Liu<sup>1,2,\*</sup> and Ju-Jun Xie<sup>2,3,†</sup><sup>1</sup>*Department of Applied Physics, Xi'an Jiaotong University, Xi'an, Shanxi 710049, China*<sup>2</sup>*Theoretical Physics Center for Science Facilities, Chinese Academy of Sciences, Beijing 100049, China*<sup>3</sup>*Department of Physics, Zhengzhou University, Zhengzhou, Henan 450001, China*

(Received 3 August 2012; revised manuscript received 16 October 2012; published 16 November 2012)

Recently, we reported a theoretical study on the  $K^- p \rightarrow \eta\Lambda$  reaction near threshold by using an effective Lagrangian approach. It was found that the description of angular distribution data measured by the Crystal Ball Collaboration needs a  $D_{03}$  resonance with mass  $M = 1668.5 \pm 0.5$  MeV and total decay width  $\Gamma = 1.5 \pm 0.5$  MeV, which is not the conventional  $\Lambda(1690)$  or other  $\Lambda$  state listed in the Particle Data Group book. In the present work, we study the  $\Lambda$  polarization in the  $K^- p \rightarrow \eta\Lambda$  reaction within the same framework. The results show that the existence of this narrow  $D_{03}$  state is also compatible with current  $\Lambda$  polarization data and that the more accurate  $\Lambda$  polarization data at  $P_{K^-} = 735$  MeV can offer further evidence for the existence of this resonance. Furthermore, the role of the  $\Lambda(1690)$  resonance in this reaction is also discussed.

DOI: [10.1103/PhysRevC.86.055202](https://doi.org/10.1103/PhysRevC.86.055202)

PACS number(s): 25.80.Nv, 13.75.Jz, 14.20.Jn

**I. INTRODUCTION**

Understanding  $\bar{K}N$  interactions in the low-energy region is a very important part of the study of the behavior of quantum chromodynamics (QCD) in the nonperturbative regime. Because the excitation of hyperon resonances usually dominates in relevant processes, it offers a good basis to study the properties of hyperon resonances, especially for hyperon resonance with  $S = -1$ . In fact, up to now most of the knowledge of hyperon resonances is from the analysis of  $\bar{K}N$  interactions [1]. Even though we have studied the  $\bar{K}N$  interactions for a long time, the large uncertainties of the parameters of hyperon resonances in the Particle Data Group (PDG) book indicate that the status of our knowledge on these resonances is still not satisfying. This is partly because of the complications of the nonperturbative character of QCD in the low-energy regime and partly because of the poor quality of the available experimental data.

In the past ten years, some new experimental data on  $K^- p$  scattering with much higher accuracy than before were reported by the Crystal Ball Collaboration [2,3]. With these new data, from theoretical analysis, it is possible to refine our knowledge on the hyperon resonances and to better understand the mechanism of relevant reactions. Some work along this way has already been done [4–9]. Among various  $\bar{K}N$  inelastic reactions, the reaction  $K^- p \rightarrow \eta\Lambda$  is particularly interesting and important. Due to isospin conservation, the  $\Sigma$  resonances do not contribute in this reaction, which makes this reaction a good place to study the properties of  $\Lambda$  resonances. On the other hand, our current knowledge of the couplings of  $\Lambda$  resonances with the  $\eta\Lambda$  channel is still very poor. Besides the  $\Lambda(1670)$  resonance, the couplings of other  $\Lambda$  resonances with the  $\eta\Lambda$  channel are only poorly known or unknown. Some further studies on this reaction are obviously still needed.

In our previous work [9], we analyzed the new data reported by the Crystal Ball Collaboration for the  $K^- p \rightarrow \eta\Lambda$  reaction

[2] within an effective Lagrangian approach. It is found that by including the background and  $\Lambda(1670)$  resonance the total cross section data can be well reproduced. However, the bowl structure appearing in the differential cross section data cannot be explained. We showed that the differential cross section data favor a  $D_{03}$  resonance with very narrow width, which is not the conventional  $\Lambda(1690)$  resonance or other  $\Lambda$  states listed by the PDG [1]. As mentioned in Ref. [9], the current experimental data still have systematic uncertainties, especially when we look at the angular distribution data obtained from two different ways of identifying the final  $\eta$  meson (see Fig. 20 of Ref. [2]). For better understanding of the origin of the higher partial wave contributions, we suggest our experimental colleagues remeasure the angular distribution data.

On the theoretical side, it is also important to find some other way or criterion to check for the existence of this narrow  $D_{03}$  resonance. In the present work, we give predictions of the  $\Lambda$  polarization in the  $K^- p \rightarrow \eta\Lambda$  reaction by using the parameters determined from the fitting to differential cross section data in our previous work [9]. On the other hand, since the conventional  $\Lambda(1690)$  resonance may also contribute to this reaction in principle, we also give some further discussion about the role of the  $\Lambda(1690)$  resonance in this reaction. The present work can be treated as a further test of our previous results [9] and offers some new criterion to verify the existence of this narrow  $D_{03}$  resonance.

The paper is organized as follows. In the next section, we present the ingredients and formalism used for the present calculation, while the results with some discussion are given in Sec. III. Then, a short summary is given in the last section.

**II. INGREDIENTS AND FORMALISM**

We adopt the effective Lagrangian method in describing the reaction  $K^- p \rightarrow \eta\Lambda$  near threshold. The effective Lagrangian method is an important theoretical approach in studying various processes in the resonance region, and it is widely used in partial wave analysis for the properties of resonances. The

\*liubc@xjtu.edu.cn

†xiejujun@mail.ihep.ac.cn

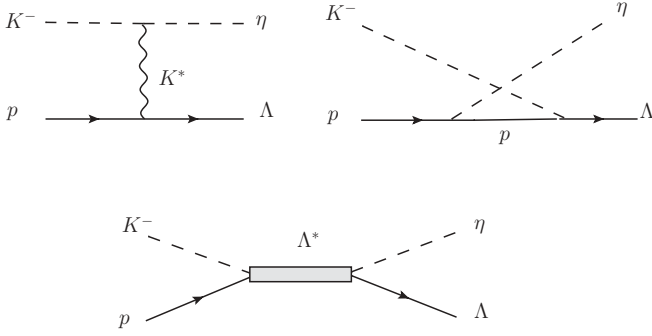


FIG. 1. Feynman diagrams for the reaction  $K^- p \rightarrow \eta \Lambda$ . The  $t$ -channel  $K^*$  meson exchange,  $u$ -channel proton exchange, and the  $s$ -channel  $\Lambda$  resonance exchange are considered.

main contributions for this reaction come from the  $t$ -channel  $K^*$  meson exchange, the  $u$ -channel proton exchange, and the  $s$ -channel  $\Lambda$  resonance exchange. The corresponding Feynman diagrams are shown in Fig. 1.

First, for the  $t$ -channel  $K^*$  meson exchange, we take the normally used effective Lagrangians for  $K^* K \eta$  and  $K^* N \Lambda$  couplings as

$$\mathcal{L}_{K^* \bar{K} \eta} = g_{K^* K \eta} (\eta \partial^\mu K^- - K^- \partial^\mu \eta) K_{\mu}^{*-}, \quad (1)$$

$$\mathcal{L}_{K^* N \Lambda} = g_{K^* N \Lambda} \bar{\Lambda} \left( \gamma_\mu K^{*\mu} - \frac{\kappa_{K^* N \Lambda}}{2M_N} \sigma_{\mu\nu} \partial^\nu K^{*\mu} \right) N + \text{H.c.}, \quad (2)$$

where we take  $\kappa_{K^* N \Lambda} = 2.43$  as used in Refs. [10,11].

Second, for the  $u$ -channel nucleon exchange, the effective Lagrangians for the  $\eta NN$  and  $KN\Lambda$  couplings are taken as [12]

$$\mathcal{L}_{\eta NN} = g_{\eta NN} \bar{N} \gamma_5 N \eta, \quad (3)$$

$$\mathcal{L}_{KN\Lambda} = g_{KN\Lambda} \bar{N} \gamma_5 \Lambda K + \text{H.c.} \quad (4)$$

Third, for the intermediate  $\Lambda(1670)$  ( $\Lambda_{\frac{1}{2}^-}^*$ ) resonance contribution in the  $s$  channel, the effective Lagrangians for the  $KN\Lambda_{\frac{1}{2}^-}^*$  and  $\eta\Lambda\Lambda_{\frac{1}{2}^-}^*$  vertices are [13]

$$\mathcal{L}_{KN\Lambda_{\frac{1}{2}^-}^*} = g_{KN\Lambda_{\frac{1}{2}^-}^*} \bar{K} \bar{\Lambda}_{\frac{1}{2}^-}^* N + \text{H.c.}, \quad (5)$$

$$\mathcal{L}_{\eta\Lambda\Lambda_{\frac{1}{2}^-}^*} = g_{\eta\Lambda\Lambda_{\frac{1}{2}^-}^*} \bar{\Lambda}_{\frac{1}{2}^-}^* \Lambda \eta + \text{H.c.} \quad (6)$$

Fourth, for the intermediate  $\Lambda^*$  resonance ( $D_{03}$  state) in the  $s$  channel with spin-parity  $J^P = \frac{3}{2}^-$ , the effective Lagrangians are [14]

$$\mathcal{L}_{KN\Lambda_{\frac{3}{2}^-}^*} = \frac{f_{KN\Lambda_{\frac{3}{2}^-}^*}}{m_K} \partial_\mu \bar{K} \bar{\Lambda}_{\frac{3}{2}^-}^{*\mu} \gamma_5 N + \text{H.c.}, \quad (7)$$

$$\mathcal{L}_{\eta\Lambda\Lambda_{\frac{3}{2}^-}^*} = \frac{f_{\eta\Lambda\Lambda_{\frac{3}{2}^-}^*}}{m_\eta} \partial_\mu \eta \bar{\Lambda}_{\frac{3}{2}^-}^{*\mu} \gamma_5 \Lambda + \text{H.c.} \quad (8)$$

To take into account the internal structure of hadrons and possible off-shell effects, we introduce form factors in the amplitudes. In the present work, we adopt the following form

factors [15–18]:

$$F_B(q_{\text{ex}}^2, M_{\text{ex}}) = \frac{\Lambda^4}{\Lambda^4 + (q_{\text{ex}}^2 - M_{\text{ex}}^2)^2} \quad (9)$$

for the  $s$  and  $u$  channels and

$$F_B(q_{\text{ex}}^2, M_{\text{ex}}) = \left( \frac{\Lambda^2 - M_{\text{ex}}^2}{\Lambda^2 - q_{\text{ex}}^2} \right)^2 \quad (10)$$

for the  $t$  channel, where  $q_{\text{ex}}$  and  $M_{\text{ex}}$  are the four-momenta and the mass of the exchanged hadron, respectively. For the cutoff parameters, we adopt  $\Lambda = 2.0$  GeV for the  $s$  channel and  $\Lambda = 1.5$  GeV for the  $t$  and  $u$  channels.

For the propagators with four-momenta  $q_{\text{ex}}$ , we take [19]

$$G_{K^*}^{\mu\nu}(q_{\text{ex}}) = \frac{-g^{\mu\nu} + q_{\text{ex}}^\mu q_{\text{ex}}^\nu / m_{K^*}^2}{q_{\text{ex}}^2 - m_{K^*}^2} \quad (11)$$

for  $K^*$  meson exchange, where  $\mu$  and  $\nu$  are polarization indices of vector meson  $K^*$ .

For the proton propagator, we take

$$G_N(q_{\text{ex}}) = \frac{\not{q}_{\text{ex}} + M_N}{q_{\text{ex}}^2 - M_N^2}. \quad (12)$$

For the  $\Lambda$  resonance with spin 1/2 in the  $s$  channel, we take

$$G_{\Lambda_{\frac{1}{2}^-}^*}(q_{\text{ex}}) = \frac{\not{q}_{\text{ex}} + M}{q_{\text{ex}}^2 - M^2 + iM\Gamma}, \quad (13)$$

while for the  $\Lambda$  resonance with spin 3/2 in the  $s$  channel, we take the propagator as

$$G_{\Lambda_{\frac{3}{2}^-}^*}^{\mu\nu}(q_{\text{ex}}) = \frac{\not{q}_{\text{ex}} + M}{q_{\text{ex}}^2 - M^2 + iM\Gamma} \left( -g^{\mu\nu} + \frac{\gamma^\mu \gamma^\nu}{3} + \frac{\gamma^\mu q_{\text{ex}}^\nu - \gamma^\nu q_{\text{ex}}^\mu}{3M} + \frac{2q_{\text{ex}}^\mu q_{\text{ex}}^\nu}{3M^2} \right), \quad (14)$$

where  $M$  and  $\Gamma$  are the mass and width of the corresponding intermediate state, respectively.

The differential cross section for  $K^- p \rightarrow \eta \Lambda$  with the invariant mass squared  $s = (p + k)^2$  (where  $k$  and  $p$  are the four-momenta of the  $K^-$  and the proton) in the center-of-mass (c.m.) frame can be expressed as

$$\frac{d\sigma_{\eta\Lambda}}{d\Omega} = \frac{d\sigma_{\eta\Lambda}}{2\pi d \cos \theta} = \frac{1}{64\pi^2 s} \frac{|\vec{q}|}{|\vec{k}|} |\bar{\mathcal{M}}|^2, \quad (15)$$

where  $\theta$  denotes the angle of the outgoing  $\eta$  relative to beam direction in the c.m. frame. In the above equation,  $|\vec{k}|$  and  $|\vec{q}|$  denote the magnitude of the three-momenta of initial and final states in the c.m. frame, respectively.

With the effective Lagrangian densities given above, the averaged scattering amplitude squared,  $|\bar{\mathcal{M}}|^2$ , introduced in Eq. (15), can be expressed as

$$|\bar{\mathcal{M}}|^2 = \frac{1}{2} \sum_{r_1, r_2} |\mathcal{M}|^2 = \frac{1}{2} \text{Tr}[(\not{p}' + m_\Lambda) \mathcal{A} (\not{p} + m_N) \gamma^0 \mathcal{A}^+ \gamma^0], \quad (16)$$

where  $r_1$  and  $r_2$  denote the polarizations of the initial proton and the final  $\Lambda$ , respectively, and  $p$  and  $p'$  denote the four-momenta of the proton and the  $\Lambda$ , respectively.  $\mathcal{A}$  is part of

TABLE I. The fitted parameters.

Channel/exchanging particle	Product of coupling constants	$\phi_\alpha$	Mass (MeV)	Width (MeV)
$s/\Lambda(1670)$	$0.3 \pm 0.03$	0.	$1672.5 \pm 1.0$	$24.5 \pm 2.7$
$s/\Lambda(D_{03})$	$28.2 \pm 7.9$	$5.66 \pm 0.47$	$1668.5 \pm 0.5$	$1.5 \pm 0.5$
$t/K^*$	$-58.0 \pm 7.2$	$2.64 \pm 0.18$	892.	–
$u/p$	$-5.3 \pm 1.0$	$2.59 \pm 0.43$	938.2	–

the total amplitude, which can be expressed as

$$\mathcal{M} = \bar{u}_{r_2}(p') A u_{r_1}(p) = \bar{u}_{r_2}(p') \left( \sum_{\alpha} \mathcal{A}_{\alpha} e^{i\phi_{\alpha}} \right) u_{r_1}(p), \quad (17)$$

where  $\alpha$  denotes the  $t$ -channel,  $u$ -channel, and various  $s$ -channel resonances that contribute to the total amplitude. In phenomenological approaches, the relative phase between the amplitudes is not fixed. In our work, they are introduced as free parameters, i.e.,  $\phi_{\alpha}$ , and we take  $\phi = 0$  for the amplitude of the  $s$ -channel  $\Lambda(1670)$  exchange.

The  $\Lambda$  polarization in the  $K^-p \rightarrow \eta\Lambda$  reaction can be studied from the decay of  $\Lambda \rightarrow \pi N$ . For  $\Lambda \rightarrow \pi N$ , we take the following effective Lagrangian:

$$\mathcal{L}_{\Lambda\pi N} = G_F m_{\pi}^2 \bar{N} (A - B\gamma_5) \Lambda, \quad (18)$$

where  $G_F$  denotes the Fermi coupling constant, while  $A$  and  $B$  are effective coupling constants, for which we take  $A = 1.762 - 0.238i$  and  $B = 12.24$  [4] in our calculation.

The differential cross section for  $K^-p \rightarrow \eta\Lambda \rightarrow \eta\pi N$  can be expressed as

$$\frac{d\sigma_{K^-p \rightarrow \eta\Lambda \rightarrow \eta\pi N}}{d\Omega d\Omega'} = \frac{|\mathbf{q}||\mathbf{p}'_n| |\bar{\mathcal{M}}'|^2}{2^{11} \pi^4 m_{\Lambda}^2 \Gamma_{\Lambda} s |\mathbf{k}|}, \quad (19)$$

where  $\mathbf{p}'_n$  is the three-momenta of the produced nucleon in the  $\Lambda$  rest frame,  $\Gamma_{\Lambda} = \tau_{\Lambda}^{-1}$  is the  $\Lambda$  decay width, and  $d\Omega' = d\cos\theta' d\phi'$  is the sphere space of the outgoing nucleon in the  $\Lambda$  rest frame. The scattering amplitude  $\mathcal{M}'$  is expressed as

$$\begin{aligned} \mathcal{M}' &= \bar{u}_{r_3}(p_n) G_F m_{\pi}^2 (A - B\gamma_5) (\not{p}' + m_{\Lambda}) \\ &\times \left( \sum_{\alpha} \mathcal{A}_{\alpha} e^{i\phi_{\alpha}} \right) u_{r_1}(p), \end{aligned} \quad (20)$$

and

$$|\bar{\mathcal{M}}'|^2 = \frac{1}{2} \sum_{r_1, r_3} \mathcal{M}' \mathcal{M}'^{\dagger}, \quad (21)$$

with  $r_1$  and  $r_3$  the polarizations of the initial proton and the final nucleon, respectively

With the above ingredients, the  $\Lambda$  polarization in  $K^-p \rightarrow \eta\Lambda \rightarrow \eta\pi N$  can be expressed as

$$P_{\Lambda} = \frac{3}{\alpha_{\Lambda}} \left( \int \cos\theta' \frac{d\sigma_{K^-p \rightarrow \eta\Lambda \rightarrow \eta\pi N}}{d\Omega d\Omega'} d\Omega' \right) / \frac{d\sigma_{\eta\Lambda}}{d\Omega}, \quad (22)$$

where  $\alpha_{\Lambda}$  is the  $\Lambda$  decay asymmetry parameter with the value of 0.65, while  $\theta'$  is the angle between the outgoing nucleon and the vector  $\mathbf{V} = \mathbf{k} \times \mathbf{q}$ .

### III. RESULTS AND DISCUSSION

In the following, we present the theoretical results of a  $\chi^2$  fit to the experimental total and differential cross section data [2] with eleven parameters ( $M_{\Lambda(1670)}$ ,  $\Gamma_{\Lambda(1670)}$ ,  $g_{\Lambda(1670)\bar{K}N} g_{\Lambda(1670)\Lambda\eta}$ ,  $M_{\Lambda(D_{03})}$ ,  $\Gamma_{\Lambda(D_{03})}$ ,  $f_{\Lambda(D_{03})\bar{K}N} f_{\Lambda(D_{03})\Lambda\eta}$ ,  $g_{K^*N\Lambda} g_{K^*K\eta}$ ,  $g_{KN\Lambda} g_{\eta NN}$ ,  $\phi_{\Lambda(D_{03})}$ ,  $\phi_{K^*}$ , and  $\phi_p$ ), which are not shown in Ref. [9] due to that paper's length limit. The best fitting results for these parameters are shown in Table I. The resultant  $\chi^2/\text{dof}$  is 0.9 (where dof is the degrees of freedom). We show in Fig. 2 the best fitting results for total cross sections by considering the  $\Lambda(1670)$ , narrow  $D_{03}$  resonance, and background contributions. The solid line represents the full results. The contributions from the  $\Lambda(1670)$ , the narrow  $D_{03}$  resonance, the  $t$ -channel diagram, and the  $u$ -channel diagram are shown by the dotted, dash-dotted, dashed, and dot-dot-dashed lines, respectively.

It was found that the  $\Lambda(1670)$  resonance is needed to interpret the steep rise of the total cross sections near threshold and a  $\Lambda(D_{03})$  state with mass  $M = 1668.5 \pm 0.5$  MeV and width  $\Gamma = 1.5 \pm 0.5$  MeV is necessary to reproduce the experimental data of the angular distributions [9]. Because of its very narrow width, this  $D_{03}$  resonance is obviously not the conventional  $\Lambda(1690)$  resonance ( $M_{\Lambda(1690)} = 1690 \pm 5$  MeV,  $\Gamma_{\Lambda(1690)} = 60 \pm 10$  MeV) or other  $\Lambda$  states listed by the PDG.

In Fig. 3 we show again our results, for comparison, for the total cross section by including the contribution from the narrow  $D_{03}$  state with a solid line and the results obtained without the narrow  $D_{03}$  state with a dashed line. It is clear

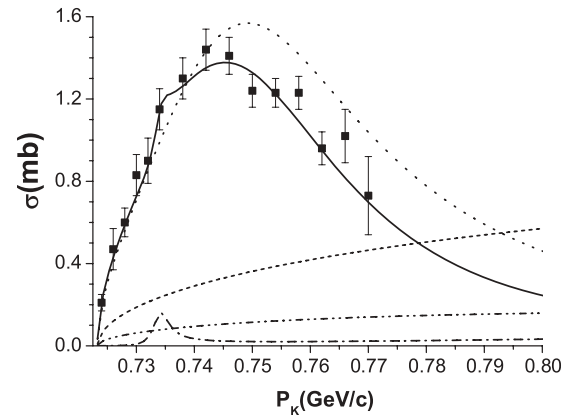


FIG. 2. The best fitting results for total cross sections by considering the  $\Lambda(1670)$ , narrow  $D_{03}$  resonance and background contributions. The solid line represents the full results. The contributions from the  $\Lambda(1670)$ , the narrow  $D_{03}$  resonance, the  $t$ -channel diagram, and the  $u$ -channel diagram are shown by the dotted, dash-dotted, dashed, and dot-dot-dashed lines, respectively.

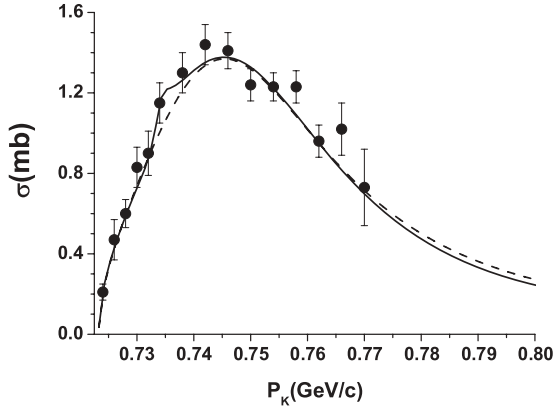


FIG. 3. Total cross section with (solid line) and without (dashed line) contributions from the narrow  $D_{03}$  state.

that the small bump around  $P_{K^-} = 734$  MeV can be well reproduced if we include the contributions from the narrow  $D_{03}$  state.<sup>1</sup>

<sup>1</sup>At the point  $P_{K^-} = 734$  MeV, the experimental result is  $\sigma = 1.15 \pm 0.10$  mb, while our model result, by including the narrow  $D_{03}$  state, is  $1.14 \pm 0.05$  mb with the error obtained from the errors of the fitted parameters shown in Table I. We find that the agreement between our model and the experimental result is very good. However,

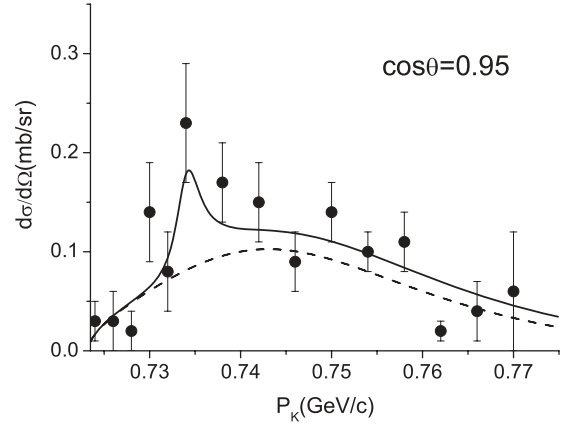


FIG. 4. Differential cross sections as a function of the momentum of  $K^-$  at the forward angle ( $\cos\theta = 0.95$ ) and the corresponding theoretical results by using the best-fitted parameters with (solid line) and without (dashed line) the narrow resonance.

To get more clues about the role of the narrow  $D_{03}$  state in the  $K^- p \rightarrow \eta \Lambda$  reaction, we calculate the differential cross

if we did not consider the contribution from this narrow  $D_{03}$  state, then the theoretical result is  $0.99 \pm 0.03$  mb, which gives discrepancies of about two standard deviations with the experimental data when the theoretical uncertainties are also taken into account.

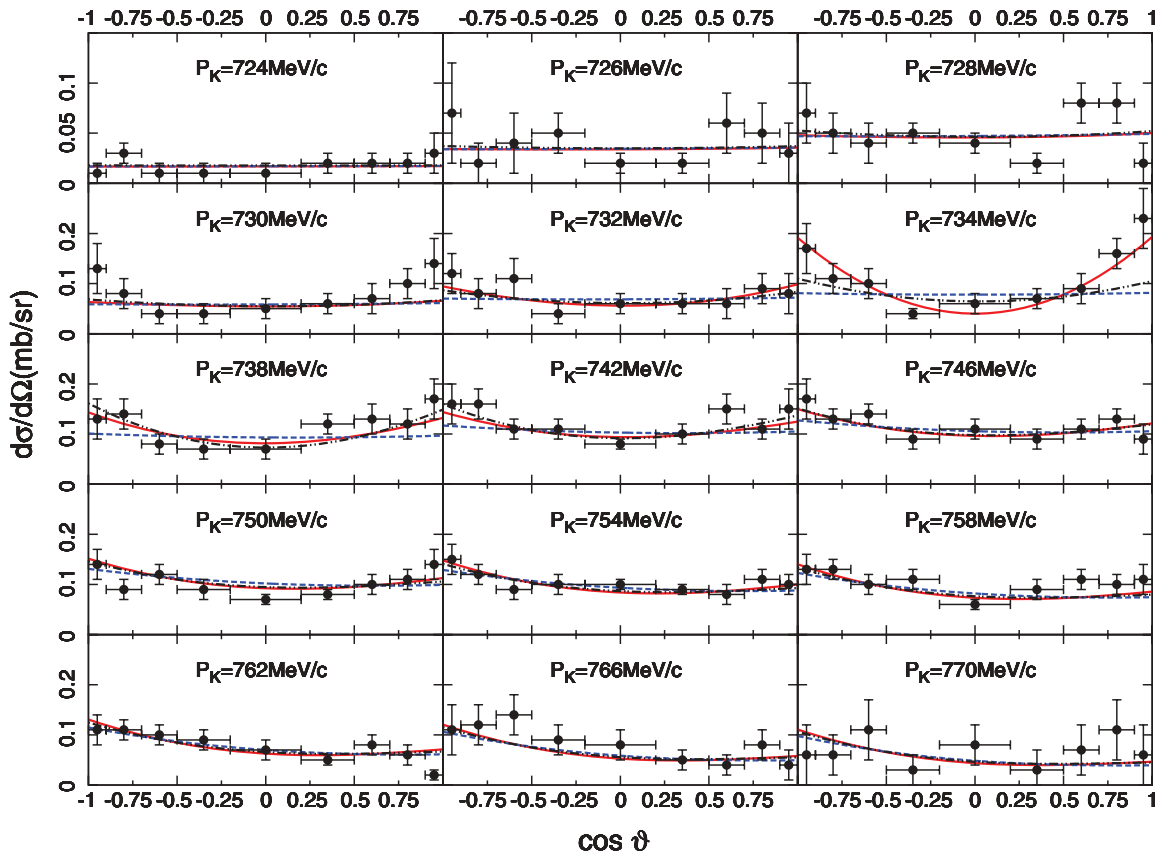


FIG. 5. (Color online) The fitting results for angular distributions within Fit I (dashed line) and Fit III (dash-dot-dotted line). The solid line represents the best fitting results taken from Ref. [9] for comparison.

sections as a function of the momentum of the  $K^-$  meson at the forward angle ( $\cos\theta = 0.95$ ). We show our results in Fig. 4 by comparing with the experimental data taken from Ref. [2]. The result including the narrow  $D_{03}$  state is shown by the solid line, while the dashed line stands for the results without including this narrow state. The bump in the differential cross section is more clear than in the total cross section, and this clear bump can be well reproduced by including the contributions from the narrow  $D_{03}$  state.

### A. The role of the $\Lambda(1690)$

It is known that a well-established  $D_{03}$  resonance [ $\Lambda(1690)$ ] may also give contributions to this reaction, and in Ref. [2], the authors argued that the bowl structure may be caused by the  $\Lambda(1690)$  resonance. However, it was shown in our previous work [9] that the experimental data favor a resonance with very narrow width. The main reason for the need of a narrow resonance is because of the bowl structures only appearing in a very narrow energy window, as we have pointed out in Ref. [9].

Regarding the uncertainties of the current experimental data, it will be interesting to discuss how well the experimental data can be explained by the conventional  $\Lambda(1690)$  state. For this purpose, we perform the fitting procedures with some different strategies. First, we fix the mass and width of the  $D_{03}$  state at the central values of the conventional  $\Lambda(1690)$  state as given by the PDG [1] (Fit I), i.e., mass  $M = 1690$  MeV and total decay width  $\Gamma = 60$  MeV. In this fit, we take the coupling of the  $\Lambda(1690)$  with the  $\eta\Lambda$  channel as a free parameter, then we have nine free parameters in total. The best fitting results are shown by the dashed line shown in Fig. 5. It is easy to see that the bowl structures cannot be reproduced. The fitting results favor a weak coupling of the  $\Lambda(1690)$  with the  $\eta\Lambda$  channel. This is mainly because the bowl structures only appear in a very narrow energy window. Since the highest c.m. energy of this set of data is around  $\sqrt{s} = 1.685$  GeV, which is the lower limit of the mass of the  $\Lambda(1690)$  suggested by the PDG, if  $\Lambda(1690)$  gives significant contributions to the angular distributions, one can expect that with increasing beam momenta the bowl structures shown in angular distributions should become more and more prominent. However, such an expectation is not supported by the experimental data. Therefore, we do not think the bowl structure is caused by the conventional  $\Lambda(1690)$ .

Another interesting thing is to check to what extent the experimental data can be understood by a  $D_{03}$  resonance with a normal total decay width. We then perform another fit by fixing the width of the  $D_{03}$  state at 60 MeV (Fit II), which is the width of the conventional  $\Lambda(1690)$  resonance suggested by the PDG. In this fit, the best fitting results favor the mass  $M = 1659.5 \pm 11.7$  MeV for the  $D_{03}$  resonance and a small coupling with the  $\eta\Lambda$  channel. The corresponding results for angular distributions are not shown in Fig. 5, because they almost overlap with the dashed-blue lines which are obtained from Fit I.<sup>2</sup> So, in this fit, the bowl structures cannot be reproduced, either.

<sup>2</sup>This is because, in both Fit I and Fit II, the  $D_{03}$  contributions are highly suppressed with the small coupling with the  $\eta\Lambda$  channel,

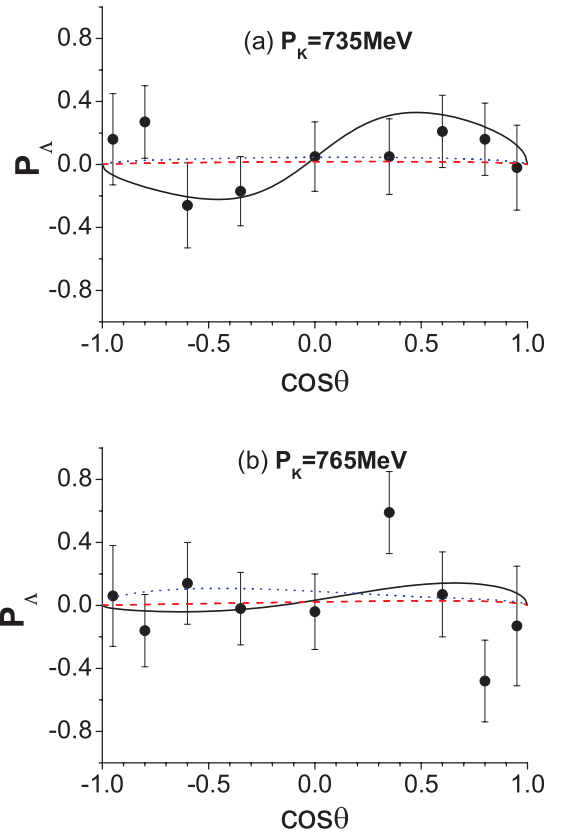


FIG. 6. (Color online) The predictions for  $\Lambda$  polarization with (solid line) and without (dashed line) the narrow  $D_{03}$  resonance. The dotted line represents the corresponding results by using the normal baryon resonance total decay width  $\Gamma = 100$  MeV for the  $D_{03}$  resonance.

Furthermore, since the bowl structure shows most significantly at  $P_K = 734$  MeV, we also check the dependence of the results on the data at this single energy point. In this scheme, we take the mass and width of the  $D_{03}$  resonance as free parameters and omit the angular distribution data at  $P_K = 734$  MeV in the fit (Fit III). The best fitting results still favor a narrow resonance, i.e.,  $M = 1670.2 \pm 1.6$  MeV and  $\Gamma = 4.5 \pm 1.6$  MeV. This shows that the needs of a narrow resonance are not only from one single energy measurement but also from the pattern of angular distributions in a wide energy region. Obviously, the description of angular distributions in this fit (shown by the dash-dot-dotted line in Fig. 5) is better than for Fit I, and also for Fit II. However, the angular distribution data at  $P_K = 734$  MeV is not totally reproduced in this fit. We also show again, in Fig. 5 by the solid-red line, the best fitting results taken from Ref. [9] for comparison.

### B. $\Lambda$ polarization

It is believed that the polarization data can put more constraints on the theoretical model and offer additional physical observables to test the models. In Ref. [9], we did

so the dominant contributions are from the  $\Lambda(1670)$  resonance and background contributions, which are similar in these two fits.

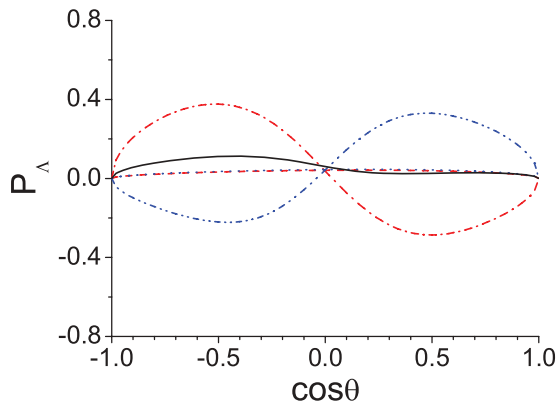


FIG. 7. (Color online) The results for  $\Lambda$  polarization at  $P_K = 733$  MeV (dash-dotted line),  $P_K = 734$  MeV (solid line), and  $P_K = 735$  MeV (dash-dot-dotted line). The dashed and dotted lines represent the corresponding results by omitting the  $D_{03}$  state contribution at  $P_K = 733$  MeV and  $P_K = 735$  MeV, respectively.

not include the  $\Lambda$  polarization data in our fitting because the quality of these data is rather poor. However, it should be meaningful to show the predictions of our fitting results for these observables. Following the formulas and ingredients given at the end of Sec. II, we calculate the  $\Lambda$  polarization in the  $K^-p \rightarrow \eta\Lambda \rightarrow \eta\pi N$  reaction at  $P_{K^-} = 735$  and 765 MeV. It should be noted that all the parameters used here are taken from Ref. [9] and there is no free parameter in the present calculation. The corresponding results are shown by the solid line in Fig. 6. The experimental data are taken from Ref. [2]. By looking at Fig. 6, one can find that the predictions of our model can fairly well describe the experimental data, especially at  $P_{K^-} = 735$  MeV, where the narrow  $D_{03}$  resonance gives a significant contribution.

It will also be interesting to check the predictions without the narrow  $D_{03}$  resonance. By using the parameters shown in Table I of Ref. [9], i.e., the best fitting results without the narrow  $D_{03}$  state, the corresponding  $\Lambda$  polarizations are calculated and shown by the dashed line in Fig. 6. It can be found that without the narrow  $D_{03}$  resonance the model predictions can also reproduce the data within the large error bars of experimental data, although the trend of central values of experimental data are described badly.

We also performed the calculations by taking a normal total decay width  $\Gamma = 100$  MeV for the  $D_{03}$  resonance and leaving other parameters unchanged. This calculation is meaningful because the  $\Lambda$  polarization is the ratio of two differential cross sections [see Eq. (22)]. The corresponding results are shown by the dotted line in Fig. 6.

Besides the predictions of  $\Lambda$  polarization at some discrete energy points, it will also be interesting to investigate the energy dependence of  $\Lambda$  polarization around the momentum

$P_K = 734$  MeV, where the narrow  $D_{03}$  resonance gives significant contributions. In Fig. 7, we show the calculated results for  $\Lambda$  polarization at  $P_K = 733$ , 734, and 735 MeV, respectively, where the predictions by omitting the contribution from the  $D_{03}$  resonance at  $P_K = 733$  and 735 MeV are also shown for comparison. The main finding is that the trend of  $\Lambda$  polarization versus  $\cos\theta$  is very sensitive to the beam momentum in the energy range around the peak of the  $D_{03}$  resonance. After omitting the contributions of the  $D_{03}$  resonance, the results at  $P_K = 733$  and 735 MeV are almost flat and overlap each other. This indicates that such energy dependence is caused by the narrow  $D_{03}$  resonance. So experimental analysis on the energy dependence of  $\Lambda$  polarization may offer further evidence on the existence of this narrow resonance.

#### IV. SUMMARY

In this work, we present some detailed analyses on the reaction mechanism of  $K^-p \rightarrow \eta\Lambda$  near threshold and study the  $\Lambda$  polarization in the  $K^-p \rightarrow \eta\Lambda$  reaction based on our previous work [9]. It is found that current data indeed favor a  $D_{03}$  resonance with very narrow width, which is not the conventional  $\Lambda(1690)$ . And the existence of this narrow  $D_{03}$  state is also compatible with the current  $\Lambda$  polarization data. We also study the role of the conventional  $\Lambda(1690)$  resonance in this reaction; however, the current experimental data cannot be reproduced by including the conventional  $\Lambda(1690)$  resonance or a  $D_{03}$  state with normal total decay width.

From the calculation of the energy dependence of the  $\Lambda$  polarization, we find that the  $\Lambda$  polarizations are strongly energy dependent around  $P_{K^-} = 734$  MeV with inclusion of the narrow  $D_{03}$  state. Thus more accurate polarization data around  $P_{K^-} = 734$  MeV can be used to verify the existence of this  $D_{03}$  resonance. We suggest our experimental colleagues remeasure both the differential cross section and  $\Lambda$  polarization data, which should be helpful to clarify the existence of this  $D_{03}$  resonance.

#### ACKNOWLEDGMENTS

We would like to thank Xian-Hui Zhong, Pu-Ze Gao, and Jia-Jun Wu for useful discussions. We also want to thank Prof. Bing-Song Zou for his valuable suggestions and support during our stay at the Institute of High Energy Physics. This work is supported by the National Natural Science Foundation of China under Grants No. 10905046 and No. 11105126. B.C.L. is also supported by the Fundamental Research Funds for the Central Universities.

- [1] J. Beringer *et al.*, *Phys. Rev. D* **86**, 010001 (2012).  
 [2] A. Starostin *et al.*, *Phys. Rev. C* **64**, 055205 (2001).  
 [3] E. Klempt and J.-M. Richard, *Rev. Mod. Phys.* **82**, 1095 (2010).  
 [4] P. Z. Gao, B. S. Zou, and A. Sibirtsev, *Nucl. Phys. A* **867**, 41 (2011).

- [5] D. M. Manley *et al.*, *Phys. Rev. Lett.* **88**, 012002 (2001).  
 [6] E. Oset, A. Ramos, and C. Bennhold, *Phys. Lett. B* **527**, 99 (2002).  
 [7] C. Garcia-Recio, J. Nieves, E. Ruiz Arriola, and M. J. Vicente Vacas, *Phys. Rev. D* **67**, 076009 (2003).

- [8] X.-H. Zhong and Q. Zhao, *Phys. Rev. C* **79**, 045202 (2009).
- [9] B.-C. Liu and J.-J. Xie, *Phys. Rev. C* **85**, 038201 (2012).
- [10] V. G. J. Stoks and Th. A. Rijken, *Phys. Rev. C* **59**, 3009 (1999).
- [11] Y. Oh and H. Kim, *Phys. Rev. C* **73**, 065202 (2006).
- [12] K. Tsushima, A. Sibirtsev, and A. W. Thomas, *Phys. Lett. B* **390**, 29 (1997).
- [13] B. S. Zou and F. Hussain, *Phys. Rev. C* **67**, 015204 (2003).
- [14] J.-J. Xie, B.-S. Zou, and B.-C. Liu, *Chin. Phys. Lett.* **22**, 2215 (2005).
- [15] F. Q. Wu, B. S. Zou, L. Li, and D. V. Bugg, *Nucl. Phys. A* **735**, 111 (2004).
- [16] J. J. Xie, B. S. Zou, and H. C. Chiang, *Phys. Rev. C* **77**, 015206 (2008).
- [17] G. Penner and U. Mosel, *Phys. Rev. C* **66**, 055211 (2002); **66**, 055212 (2002); V. Shklyar, H. Lenske, and U. Mosel, *ibid.* **72**, 015210 (2005).
- [18] T. Feuster and U. Mosel, *Phys. Rev. C* **58**, 457 (1998); **59**, 460 (1999).
- [19] R. Shyam, *Phys. Rev. C* **60**, 055213 (1999).